A quantitative Test of the **Applicability of Independent Scattering to High Albedo Planetary Regoliths**

by

Jay D. Goguen

Jet Propulsion Laboratory/California Institute of Technology
Mail Stop 183-501
4800 Oak Grove Drive
Pasadena, CA 91109

Telephone: (818) 354-8748
E-mail: jdg@scn5.jpl.nasa.gov (Internet)

22 March 1993

(To be submitted to Icarus)

Number of Pages: 14
Number of Figures: 4
Number of Tables: 0

Proposed Running Head: Scattering in High Albedo Regoliths

Editorial Comments and Proofs should be sent to:

Jay D. Goguen

Mail Stop 183-501
Jet Propulsion Laboratory
4800 Oak Grove Drive
Pasadena, CA 91109

Abstract

To test the hypothesis that the independent scattering calculation widely used to model radiative transfer in atmospheres and clouds will give a useful approximation to the intensity and linear polarization of visible light scattered from an optical l y thick *surface* of *transparent* particles, laboratory measurements arc compared to the independent scattering calculation for a surface of spherical particles with known optical constants and size (Distribution. Because tbc shape, size distribution, and optical constants of the particles arc known, the independent sc.altering calculation is completely determined and the only remaining unknown is the net effect of the close packing of the particles in the laboratory Sample Surface. 'l'he size distribution and porosity of the surface arc chosen to bc similar to those for the particles that dominate visible light scattering in the lunar regolith. The linear polarization measurements arc well matched by the independent scattering calculation. Qualitatively, the intensity calculations and measurements exhibit similar overall shape and agree quantitatively at phase angles near 10 degrees. But at moderate to large phase angles, especially for 60 degrees emission angle, the calculated intensities exceed the measured intensities by >20%. This difference is a measurement of the net effect of close packing of particles in a high albedo surface which should be of interest to a number of researchers. Overall, wc conclude that the independent scattering calculation gives a good approximation to the. linear polarization and a useful estimate of the intensity, when the moderate effects of c1osc packing arc recognized. The independent scat tering calculation should prove to bc a useful tool for extracting quantitative information on particle composition and size distribution from photometric, polarimetric, and spectral remote sensing measurements of tbc high albedo regoliths of some icy satellites in the outer solar system. An appendix shows that the backward scattered intensity is significantly underestimated if the isotropic multiple scattering approximation is used instead of the exact doubling calculation for multiple scattering by these anisotropic particle phase functions.

Introduction

One of the most important techniques for studying the planetary surfaces is quantitative measurement and interpretation of the light scattered from them. Both ground-based observations and spacecraft reconnaissance of solar system bodies contribute to the rapidly accumulating database of planetary surface photometry and polarimetry. Like the lunar surface, many planetary surfaces consist of an optically thick layer of particulate debris, or regolith, that is the net result of impact processes working the surface. Consequently, models that quantitatively describe the scattering of light by particulate surfaces are of fundamental importance to planetary science.

in a planetary atmosphere, the gas molecules, aerosol and cloud particles are sufficiently well separated that they can be assumed to scatter "independently". Van de Hulst (1957) estimates that a mean interparticle distance of 3 times the particle radius is a "sufficient condition for independent scattering". when independent scattering is valid, each particle resides in the "far-field" radiation pattern of its neighbors and the electric and magnetic field vectors add incoherently without regard to phase differences. Established radiative transfer techniques can be used to calculate the intensity and polarization of scattered light measured by a remote observer (e.g. Chandrasekhar, 1960; Hansen and Travis, 1974).

In a planetary regolith, the particles are supported by physical contact with their neighbors. If they are much larger than a wavelength and have significant opacity, they can cast shadows on each other and the independent scattering assumption is not applicable. Hapke (1963, 1966, 1981, 1986) and Irvine (1966) report techniques for including interparticle shadowing in scattering calculations. Much attention has recently focused on "coherent backscatter" (Hapke, 1990; Mishchenko, 1992; Peters 1992), a phenomenon related to the breakdown of independent scattering conditions at very small phase angles. It is a compelling explanation of the unusual radar properties of the Galilean satellites. At visible wavelengths, it may be responsible for the strong surge in the brightness of Titania and Oberon at phase angles < 0.5 degree (Hapke, 1990).

To produce the high albedo regoliths of the icy satellites of the outer planets, e.g. Enceladus, Triton, and Europa, the particles must be transparent. Addition of even minute amounts of a strongly absorbing component will reduce the surface albedo substantially (Clark, et al. 1984). For these high albedo regoliths,

it is questionable whether either independent scattering or interparticle shadowing is applicable.

in this paper, wc quantitatively test the degree to which the independent scattering calculation approximates the *intensity and linear polarization* of light scattered from a high albedo particulate surface. To accomplish this, wc perform a controlled experiment. For an optically thick layer of glass spheres several pm in radius, with known optical constants and a known size distribution, wc rigorously calculate the intensity and linear polarization of scattered light assuming independent scattering. We then measure the intensity and polarization of light scattered from a sample surface of these spheres. A comparison of the calculations and measurements provides the answers to 2 important questions: 1) For an actual particulate surface with a size distribution of transparent particles whose mean size and spacing arc similar to particles in the lunar regolith, dots the scattered intensity and linear polarization of visible light qualitatively resemble the independent scattering calculation? 2) What is the magnitude and character of the differences between the calculation and the measurements?

Samples and Measurements

The particles used in the test sample arc Uniform Glass Microspheres purchased from Duke Scientific Corporation of Palo Alto, CA, Catalog Number 146B. They arc soda-lime glass high-quality spheres with a size distribution characterized by a mean radius 4.0μm+/-0.9 μm (standard deviation). 'l'his size is chosen to bc similar to the mean scattering radius for visible light scattered by particles in the lunar regolith, 3<rsca<8μm (Goguen, 1992). These particles arc still large compared to the wavelength and have the size parameter in the Mic calculation, $x = 2\pi r/\lambda$, in the range x=43+-/-19. The complex index of refraction as supplied by the manufacturer is

$$n - ik = 1.51 - i3.2e\text{-}6 \quad (\lambda = 0.589\mu m)$$

The specific gravity of the glass is 2.4-2.5.

The sample dish is cylindrical, 1.27 cm in radius and 1.27 cm deep. A level surface was formed without compacting the sample. The sample dish was filled with particles, then a straight-edge was moved across the rim of the sample dish to obtain a flat base surface. The topmost fcw mm were added by

dusting this flat surface with an even coating of particles from a sieve. The mean density of the sample layer was 1.07 g/cc, which corresponds to a porosity (ratio of the specific gravity of the glass to the sample mean density) of 0.44. This is similar to the porosity of the uppermost few mm of the lunar surface determined from in situ measurements (Carrier et al., 1973).

To test the optical thickness of the sample layer, measurements were made with 2 different sample dishes: one with a white bottom surface and another with the bottom painted flat black. Measurements made with the detector viewing the surface along its normal, emission angle ε=0 degrees, and incidence angle ι= 4 degrees showed the difference in the reflectance of these 2 samples to be <0.5%, the precision of the measurements. Based on this test, the sample surface is presumed to have infinite optical depth.

The Cornell Goniometer (Goguen, 1981) was used to measure the intensity and linear polarization of light reflected from the sample over a wide range of scattering geometries. Two positions of the detector were used, ε=0 and ε=60 degrees. ι was varied to scan the largest possible range of phase angle, et, with the light source, detector and sample surface normal coplanar. Practical considerations limit the range to $4<\alpha<70$ degrees for ε=0 and to $4<Y,<130$ degrees for ε=60 degrees. The light source housing begins to block the detector field-of-view at $\alpha<4$ degrees. The wavelengths reaching the detector were limited to a narrow passband centered at λ=0.589μm with $\Delta\lambda/\lambda$=0.03.

I/F is a convenient dimensionless unit for reporting the intensity. I lere the incident collimated beam has flux πF crossing a plane perpendicular to its propagation direction and I is the intensity of the scattered light. The absolute calibration of 1/1' depends on the assumption that I/F for a reference standard sample is cos ι at a single scattering geometry for for each of the 2 detector positions. Specifically, for ε=0 and ι=30 degrees and for ε=60, ι=4, and (x=64 degrees. The reference standard was a surface painted with BaSO4 (Kodak Paint #6080). At all other geometries, I/F was scaled by the ratio of the photon counting rate (with the chopped background subtracted) to that at the reference geometry. 'l'his approach was adopted because the direct measurements of the reference surface show that it deviates from cos ι behavior by -10% at α<15 degrees and near the specular point. The stability of the counting rate was tested by multiple observations at the same geometry at the start, during, and at the end of each run. The absolute calibration of I/F is reliable to ~10%. The integration time was sufficient to record -] 0,000 photon-counts so that the statistical error in each data point is –1 %.

The measurement sequence consisted of 3 measurements through a sheet-type polarizer at O, 45, and 90 degree orientations. Absolute calibration of the polarization measurements was confirmed by measuring the 1 ()()% linear polarization of light scattered from a liquid distilled water sample at the Brewster angle.

Independent Scattering Calculations

11 the particles scatter independently, the intensity and linear polarization of an optically thick layer can be predicted from first principles using Mie theory and the "doubling method" used in atmospheric radiative transfer calculations (Hansen and Travis, 1974).

The first step in this calculation is to integrate the Mic scattering contributions for each particle size over the size distribution to determine the mean phase function and line.ar polarization for a unit volume of the particles. The Mic scattering program given in Hansen and Travis (1974) was used to perform this calculation for the size distribution of the Duke glass microspheres cited above. In the program, the size distribution was represented as log-normal with rg=3.5354μm and σg=0.2222 which arc the log-normal size distribution parameters that correspond to the mean particle size and standard deviation of the distribution supplied by the manufacturer. The important particle size parameter in the Mic calculation is the ratio of the particle circumference to the wavelength of light. For this reason, the width of the particle size distribution and the bandwidth of the filter have similar effects on the calculations. in this case and in many other cases of practical interest (Goguen, 1992)

$$\sigma/\langle r\rangle \gg \Delta\lambda/\lambda$$

and the effects of the finite filter bandwidth arc negligible in comparison to the effects of the broad particle size distribution. The mean phase function and linear polarization, the components of the phase matrix used in the doubling calculation below, for tbc volume *average* "single" scattering arc shown in fig. 1, for n=1.51, k=3.2e-6, and λ=0.589μm. The single scattering albedo is w=0.9997 and the anisotropy parameter is g=+0.786.

As is evident from fig. 1, the particles scatter anisotopically. The -11 magnitude range of the mean phase function corresponds to a factor of ~25,000 with most of the range contained in the forward scattering peak that is confined to co170 degrees. Such phase functions with strong forward and backward

scattering peaks are typical of transparent and semi-transparent spherical particles that are large compared to λ. The linear polarization shows a "negative branch" at small α, a strong "rainbow" feature which peaks near α=17 degrees, and comparatively neutral polarization at moderate to large α.

Multiple scatter-ing can be rigorously treated for anisotropic particles that scatter independently using the "doubling method" (Hansen and Travis, 1974). Fortran programs written to perform the doubling calculation including linear polarization for atmospheric radiative transfer calculations (POLDUB and POLMULT, R. A. West, personnal communication) were modified for application to the case of an optically thick layer of anisotropic scatterers. The program POLDUB takes the phase matrix that is the output from the Mic scattering calculations and performs the doubling calculation to generate as output the R-matrix that describes reflection from an optically thick layer (τ= 1024). Based on the POLMULT program that was designed to model a series of multiple layers of differing optical depths, a new routine, POLSCAT, was created that calculates the intensity and polarization for an arbitrary scattering geometry from a single optically thick layer given the R-matrix as input. Once the POLDUB program is run and the R-matrix output file is generated, POLSCAT rapidly calculates the intensity and linear polarization for any set of geometries of interest.

Two important parameters in the POLDUB calculation are the number of Gaussian ordinates and the number of Fourier coefficients. The Gaussian ordinates are used in the calculation of the zenith angle integrals and more terms are needed to describe scattering by more anisotropic phase functions (Hansen and Travis, 1974). The Fourier terms are used to describe the azimuthal variations. For accurate treatment of the detailed structure and anisotropic character of phase matrices like those shown in fig. 1, 50 Fourier terms and 48 Gaussian ordinates were used.

To demonstrate convergence of the doubling solution, fig. 2 compares the solutions obtained for the cases of 32 and 48 Gaussian ordinates and 50 Fourier coefficients. The major differences are in the intensity at α<5 degrees. Small differences also occur in the polarization for α<15 degrees in the ε=0 case. For all other scattering geometries relevant to this study, the intensities and polarizations calculated with 32 and 48 Gaussian ordinates are nearly identical.

These calculations were performed on a Sun4 processor and require approximately 30 hours of cpu time for 48 Gaussian ordinates. The cpu time required is proportional to the square of the number of ordinates. The R-matrix output

file occupies ~8 Mb. For the remaining calculations and discussion, we will use 48 Gaussian ordinates and 50 Fourier terms.

Comparison of measurements and calculations

Fig. 3 compares the results of the calculations to the goniometer measurements. A "prediction" (Appendix A) calculation was done prior to making the measurements so that the geometric sampling would be adequate to detect the anticipated intensity and polarization features. The basic features of the calculations are reproduced in the measurements, both for $\varepsilon=0$ and $\varepsilon=60$ degrees.

In the intensity, the 2 maxima at $\alpha<20$ degrees predicted by the calculations are seen in the data at the expected geometries. For $\varepsilon=0$, the second intensity peak near $\alpha=17$ degrees is smaller than the calculated peak and for $10<\alpha<60$ degrees, the measured intensity is IO-2(F% less than the calculated intensity. For $\varepsilon=60$ degrees, the 20-30% decrease in the calculated intensity at $\alpha=5$ degrees, compared to the intensity at $\alpha=5$ degrees and $\varepsilon=0$ degrees, is measured indicating that the ι and ε dependence of the independent scattering approximation is reasonable. At $\alpha>40$ degrees, the measured intensity is 10 to as much as 40% (at $\alpha=130$ degrees) less than the calculated intensity.

in the polarization, both the predicted "negative branch" at $\alpha<1O$ degrees and the positive maximum at $\alpha\sim15$ degrees are quantitatively reproduced in the $\varepsilon=0$ measurements. Even the predicted significant increase in the polarization maximum between the $\varepsilon=0$ and $\varepsilon=60$ degree geometries is seen in the data. The only significant discrepancies between the calculated anti measured polarization are that the measured peak polarization of the rainbow is not as large as predicted and the small polarizations for $\alpha>90$ degrees with $\varepsilon=60$ degrees are somewhat larger than those calculated.

Discussion

Fig. 3 shows that the *exact* calculation of independent scattering can be expected to give an excellent quatitative prediction of the linear polarization and a useful approximation to the intensity of light scattered from high albedo planetary regoliths. The specific case tested uses a sample with porosity similar to the lunar regolith and particles of a similar mean size to those that dominate visible wavelength light scattering in the lunar regolith. This conclusion can be

expected to be valid for transparent particles that are large compared to the wavelength and porosities that arc smaller than or approximately equal to 0.4. Specifically, this result should *not* depend on the particle shape, the values of the optical constants, or the wavelength of light as long as the particles arc transparent and large compared to the wavelength.

The degree of mismatch between the calculations and the data in fig. 3 is interpreted as a *measurement* of the net effect of close-p:ickitlg of the particles. Future efforts at modelling scattering by close-packed transparent particles may find this mismatch to be an important data set which suggests physical mechanisms that may be responsible for the effect. Note that this mismatch dots *not* resemble the enhanced backscattering behavior that characterizes the models of interparticle shadowing (e.g., Hapke, 198 1; Irvine 1966) that pertain to regoliths of large opaque particles. Future work that compares the independent scattering calculation to measurements (m samples of different porosities is suggested.

Appendix A compares the rigorous calculation of multiple scattering by these anisotropic particles to the result obtained using the popular isotropic multiple scattering approximation. For anisoptropic phase functions with both forward and backward scattering peaks, approximating the multiple scattering as that for isotropic particles results in a significant underestimation of the backward scattered intensity (fig. Al).

The only physical characteristics of the "regolith" used to calculate both the intensity and linear polarization in this test were the size distribution and optical constants of the glass spheres. For other large transparent particles with shapes and orientations for which the phase matrix can be determined, the independent scattering calculation can be expected to give useful results similar to this test case. The experiment and calculations described here are an important first step towards a model that should enable reliable quantitative information on the composition and size distribution of particles in high albedo regoliths to be deduced from photometric, spectroscopic, and polarimetric measurements.

Appendix A. The Isotropic Multiple Scattering Approximation

Some widely used models for scattering in planetary regoliths (e.g., Hapke, 1981 ; Goguen, 198 1) approximate the multiple scattering component of the intensity as that for isotropic scattering. in this isotropic multiple scattering

(lMS) approximation, the single scattering is calculated exactly and higher orders of scattering are approximated by isotropic scattering using the H-functions for isotropically scattering particles with the same single scattering albedo (Chandrasekhar, 1960). This approach has the distinct advantage that the calculation is fast and easy. Hapke (1981) gives a convenient and simple analytic expression that approximates the isotropic Ii-functions within a few percent.

in this paper, the exact calculation of multiple scattering for a realistic single particle phase function provides an opportunity to quantitatively test the accuracy of the IMS approximation for surfaces of *high albedo particles with anisotropic phase functions with both forward and backward scattering peaks.* Because this test involves only a comparison of the exact and approximate *calculations*, the goniometer measurements will not be discussed further in this appendix.

An obvious extension of the lMS approximation wil be made to include an estimate, of the linear polarization. Let

$$J = P11(\alpha) + H(\mu)H(\mu 0) - 1 \quad (A1)$$

where P11(α) is the single particle phase function that is the first element of the phase matrix derived from the Mic scattering calculation, H is the H-function for isotropic scattering evaluated for the particle albedo w, μ and $\mu 0$ are the cosines of the. emission and incidence angles, respectively, and α is the phase angle. Then the IMS approximation forth intensity is

$$I/F = (w/4)\,\mu 0/(\mu+\mu 0)\,J \quad (A2)$$

and for the linear polarization

$$p = -P21\ (et)\ /\ J \quad (A3)$$

where the multiple scattering component is assumed unpolarized and P21 (et) is the linear polarization component of the phase matrix also derived from the Mic scattering calculation (Hansen and Travis, 1974). Fig. Al compares the exact calculation obtained using the doubling method to the IMS approximation for both the intensity and linear polarization of λ=0.589μm light scattered from the size distribution of glass spheres described in the text.

For both emission angles, the IMS approximation significantly underestimates

the exact calculation of the intensity at phase" angles <30 degrees. As a consequence, any mode] that assumes IMS and attempts to match the intensity at <30 degrees phase angle will be forced to enhance the backscattered component using other model parameters to compensate for the approximate treatment of multiple scattering.

The 1 MS approximation to the linear polarization (eq. A3) qualitatively matches the exact calculation with the major difference between them being the smaller maximum polarization of the rainbow feature in the 1 MS approximation.

Acknowledgements

The author gratefully acknowledges contributions from R. A. West, who provided FORTRAN programs for the doubling calculation including polarization that were the starting point for these calculations, J. Veverka for access to the Cornell Goniometer, D. Kane of Duke Scientific, inc. for assistance in the detailed (inscription of the glass particles, and P. J. Goguen for sharing various sources, (inscriptions, and samples of commercial spherical particles.

References

Carrier, W. D., J. K. Mitchell, A. Mahmood (1973). The relative density of lunar soil. Fourth Lunar Sci. Conf., Geochim. Cosmochim. Acts. Suppl. 4, Vol. 3, 2403-2411.

Chandrasekhar, S. (1960). Radiative Transfer. Dover, New York.

Clark, R. N. and P. G. Lucey (1984). Spectral properties of icc-particulate mixtures and implications for remote sensing. Icarus 49, 244-257.

Goguen, J. D. (1981). A theoretical and experimental investigation of light scattering by particulate surfaces. Ph.D. Thesis, Cornell University.

Goguen, J. (1992). Light scattering by lunar-like particle size (distributions. lunar and Plan. Sci. Conf XXIII, 419-420.

Hansen, J. E., and Travis, L. (1974). Light scattering in planetary atmospheres. Space Sci. Rev. 16, 527-610.

1 Iapke, B. W. (1963). A theoretical photometric function for the lunar surface. J. Geophys. Res. 68, 4571-4586.

Hapke, B. W. (1966). A n improved lunar theoretical photometric function. Astron. J. 71, 333-339.

Hapke, B. W. (1981). Bidirectional reflectance spectroscopy. 1. Theory. J geophys. RCS. 86, 3039-3054.

1 Iapke, B. W. (1 986). Bidirectional reflectance spectroscopy. 4. The extinction coefficient and the opposition effect. Icarus 67, 264-280.

Hapke, B. W. (] 990). Coherent backscatter and the. radar characteristics of outer planet satellites. Icarus 88, 407-417.

Irvine, W. M. (1 966). The shadowing effect in diffuse reflection. J. Geophys. Res. 71, 2931 -2937.

Mishchenko, M. 1. (1992). Polarization characteristics of the coherent backscatter opposition effect. Earth, Moon, and Planets 58, 127-144.

Peters, K. J. (1 992). Coherent-backscatter effect: A vector formulation accounting for polarization and absorption effects and small or large scatterers. Phys. **Rev.** B 46, 801-812.

Van de Hulst, **11.** C. (1957). Light Scattering by Small Particles. Wiley, New York.

Figure Captions

Fig. 1. Mie scattering calculations of the mean phase function (a) and linear polarization (b) for "single scattering" by the size distribution of glass spheres described in the text with n=1.51, k=3.2e-6, and λ=0.589μm.

Fig. 2. Comparison of the calculated intensity and linear polarization for an optically thick layer of the size distribution of the glass spheres using 50 Fourier terms and 32 (dashed line) and 48 (solid line) Gaussian oridinates. a) Intensity for ε= O; b) Polarization for ε=0; c) Intensity for ε=60 degrees; d) Polarization for ε=60 degrees.

Fig. 3. Comparison of the calculated intensity (I/F) and linear polarization assuming independent scattering (solid line) to the goniometer measurements (points) for the sample high albedo "regolith" of glass spheres. a) Intensity for ε=0; b) Polarization for ε=0; c) Intensity for ε=60 degrees; d) Polarization for ε=60 degrees.

Fig. A 1. Comparison of the doubling calculation of the intensity (I/F) and linear polarization (solid line) to the isotropic multiple scattering approximation (eqs. A 1 -A3) for the intensity and polarization for the phase matrix elements shown in fig. 1. a) Intensity for ε=0; b) Polarization for ε=0; c) Intensity for ε=60 degrees; d) Polarization for ε=60 degrees. Notice that the IMS approximation underestimates the backscattered intensity for these anisotropically scattering particles.

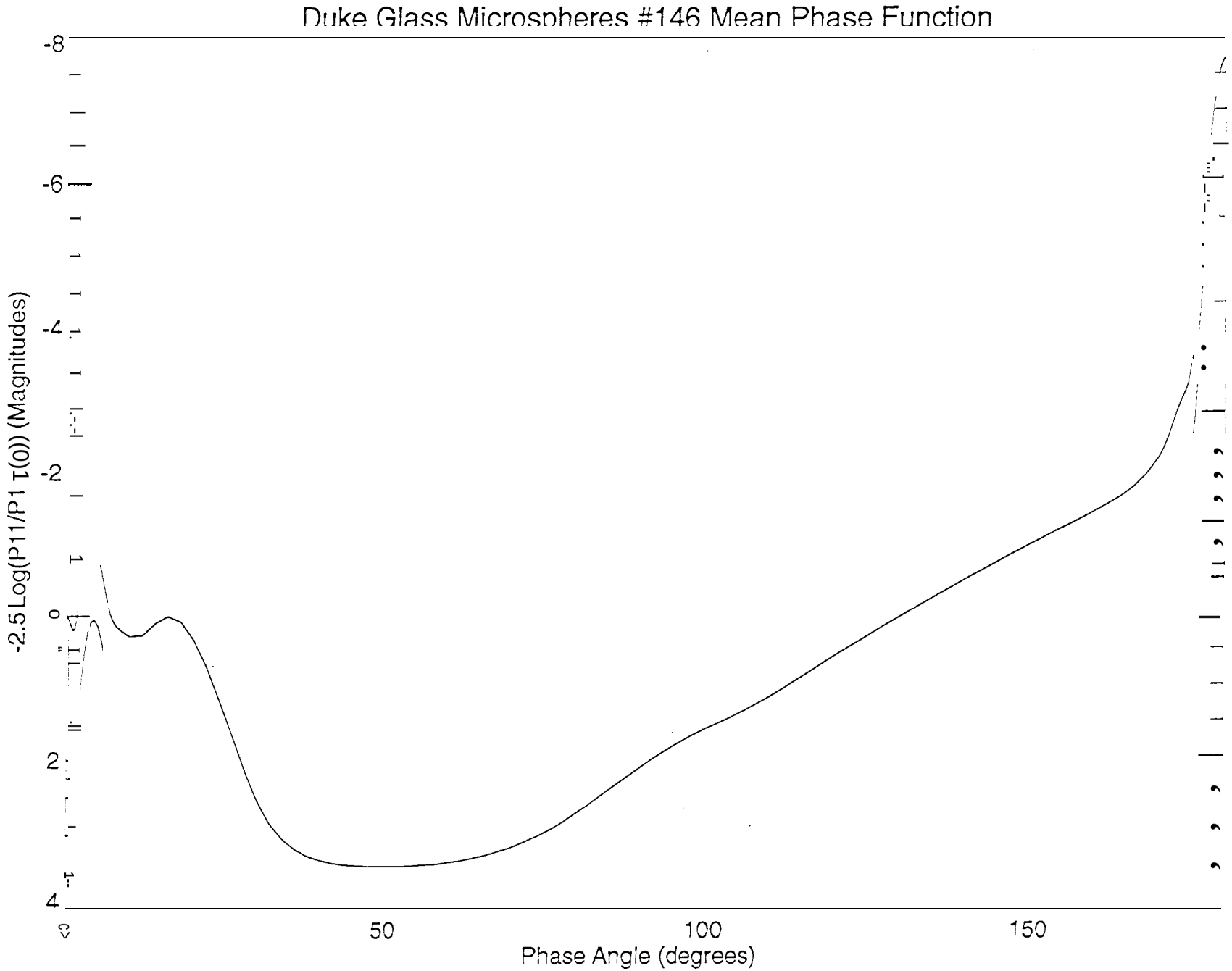
Duke Glass Microspheres #146 Mean Phase Function
-2.5 Log(P11/P1 τ(0)) (Magnitudes)
-8
-6
-4
-2
0
2
4
0
50
100
150
Phase Angle (degrees)

Fig. 1a

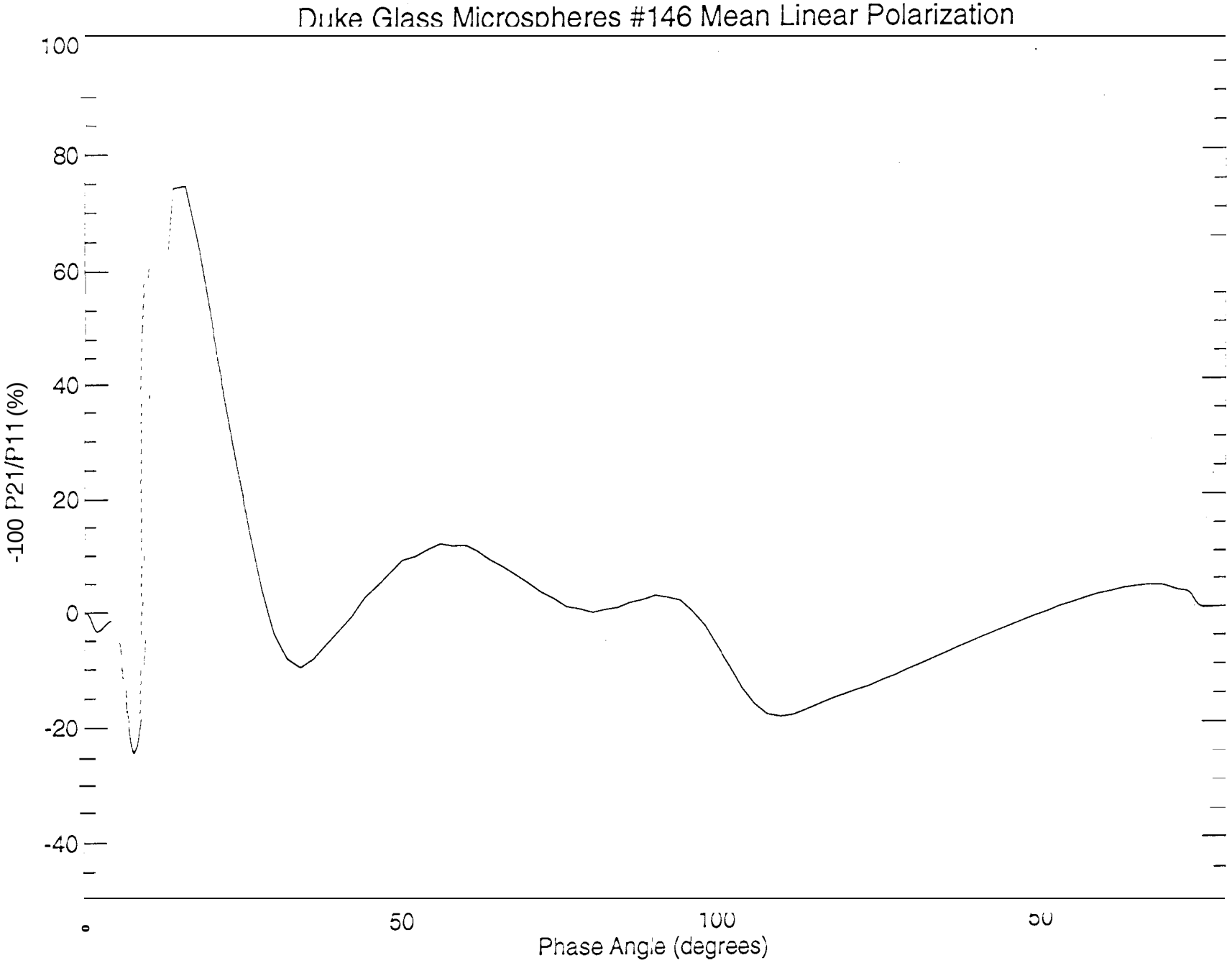
Duke Glass Microspheres #146 Mean Linear Polarization
100
80
60
40
20
0
-20
-40
-100 P21/P11 (%)
0
50
100
150
Phase Angle (degrees)

Fig. 1b

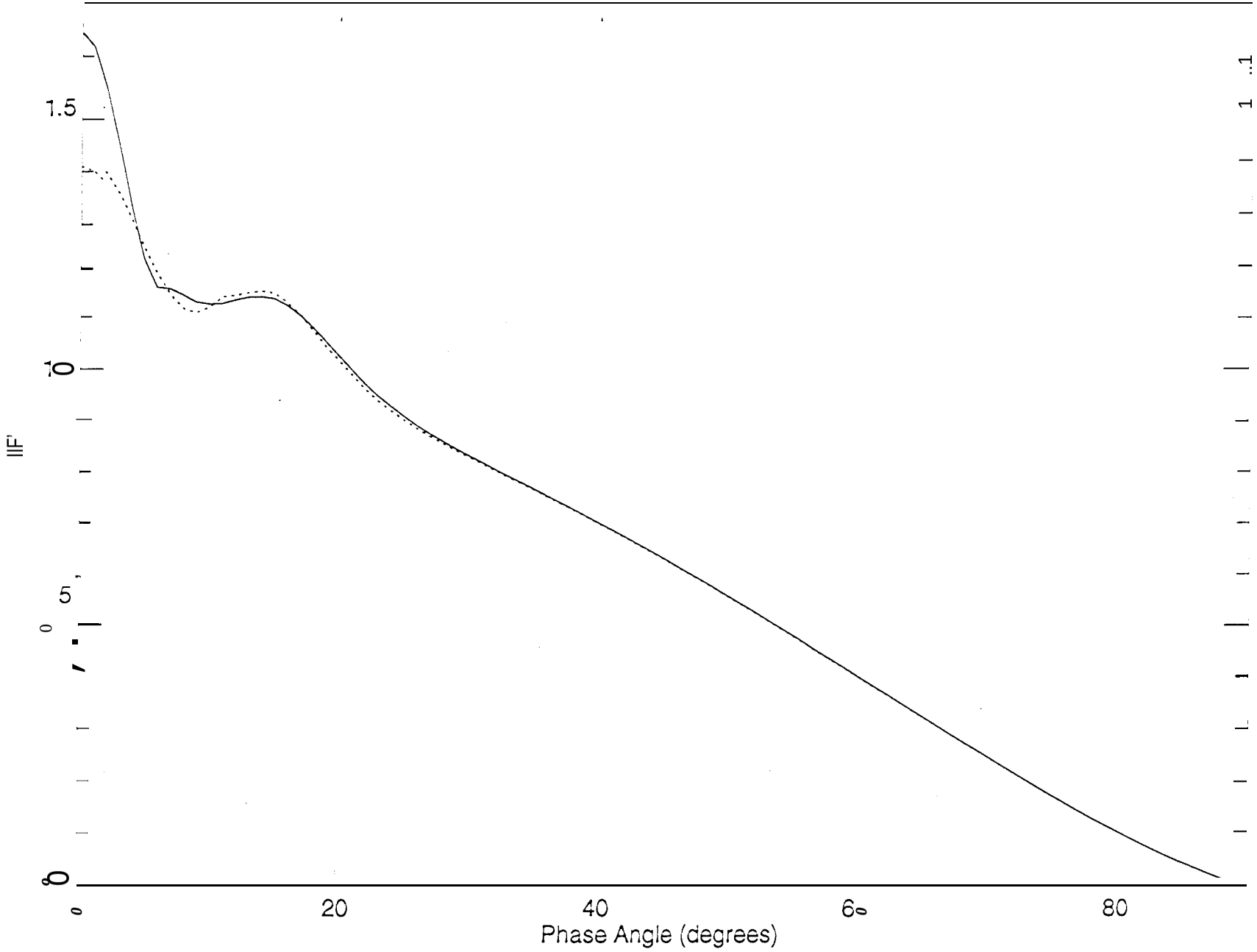
Comparison of 32 & 48 Gaussian Ordinates (50 Fourier Terms, e=0)
1.5
1
0.5
0
IIF'
0
20
40
60
80
Phase Angle (degrees)

Fig. 2a

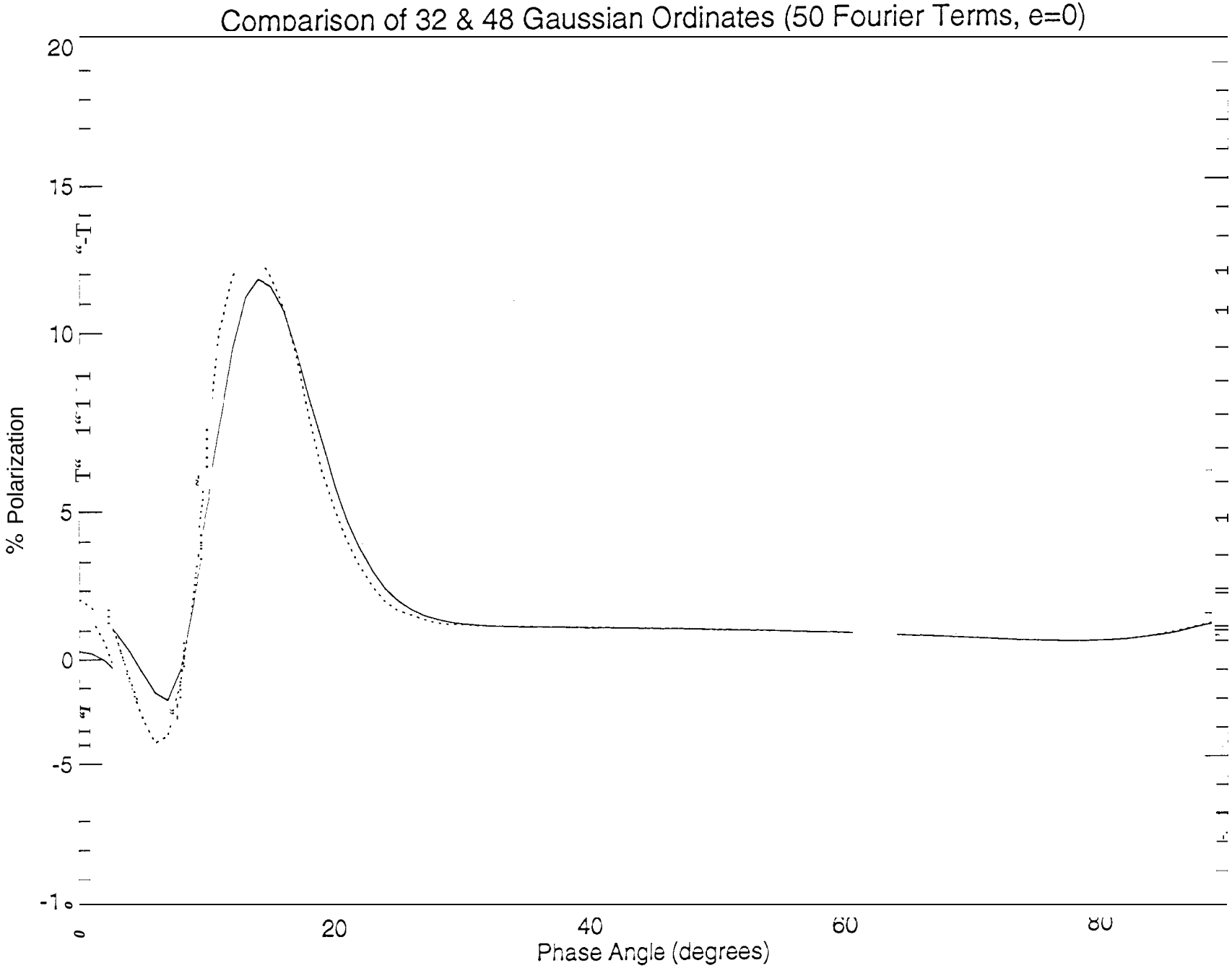
Comparison of 32 & 48 Gaussian Ordinates (50 Fourier Terms, e=0)
% Polarization
Phase Angle (degrees)
20
15
10
5
0
-5
-1
0
20
40
60
80

Fig. 25

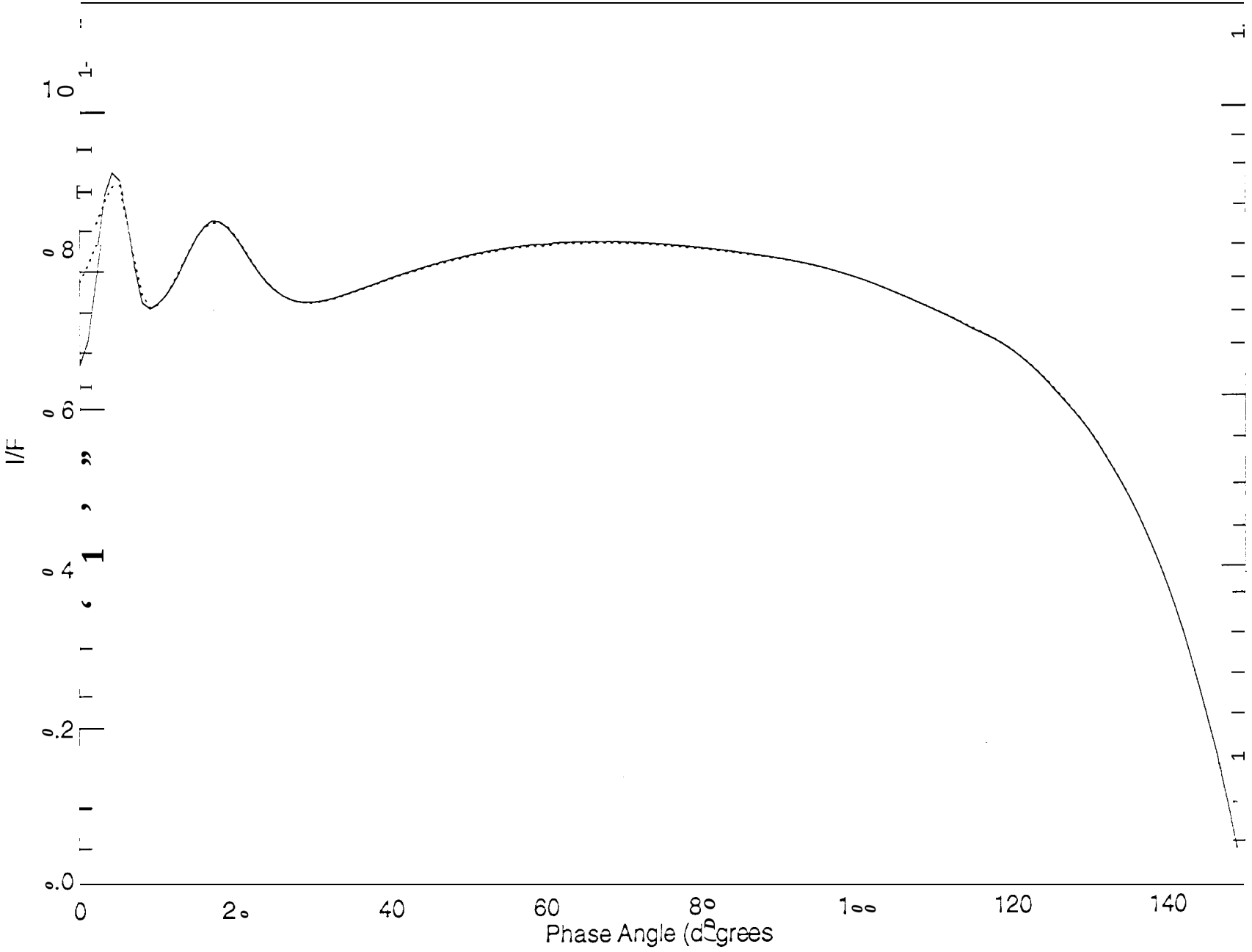
Comparison of 32 & 48 Gaussian Ordinates (50 Fourier Terms, e=60)
I/F
1.0
0.8
0.6
0.4
0.2
0.0
0
20
40
60
80
100
120
140
Phase Angle (degrees

Fig. 2c

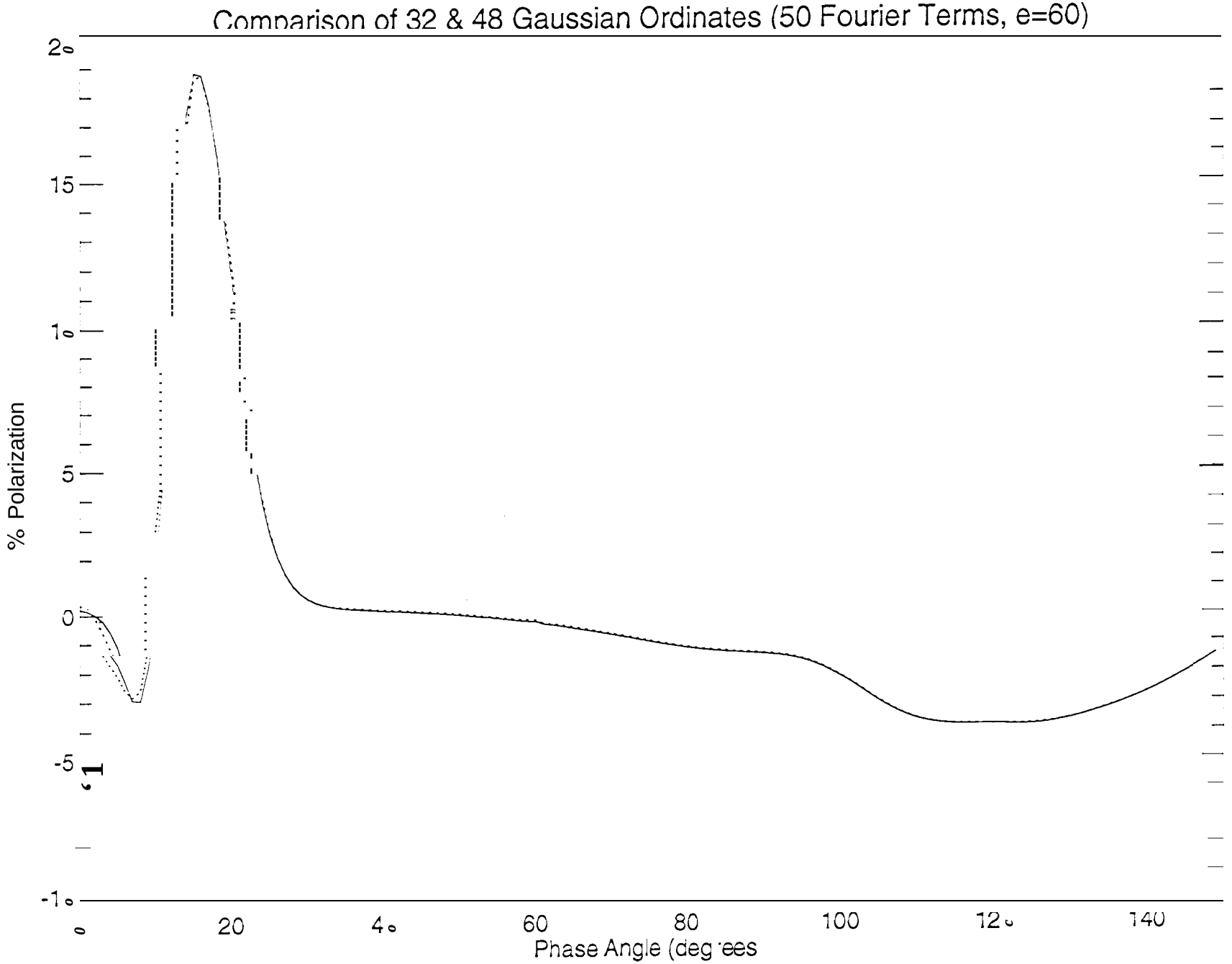
Comparison of 32 & 48 Gaussian Ordinates (50 Fourier Terms, e=60)
% Polarization
Phase Angle (degrees)
20
40
60
80
100
120
140
15
10
5
0
-5
-10

Fig. 2d

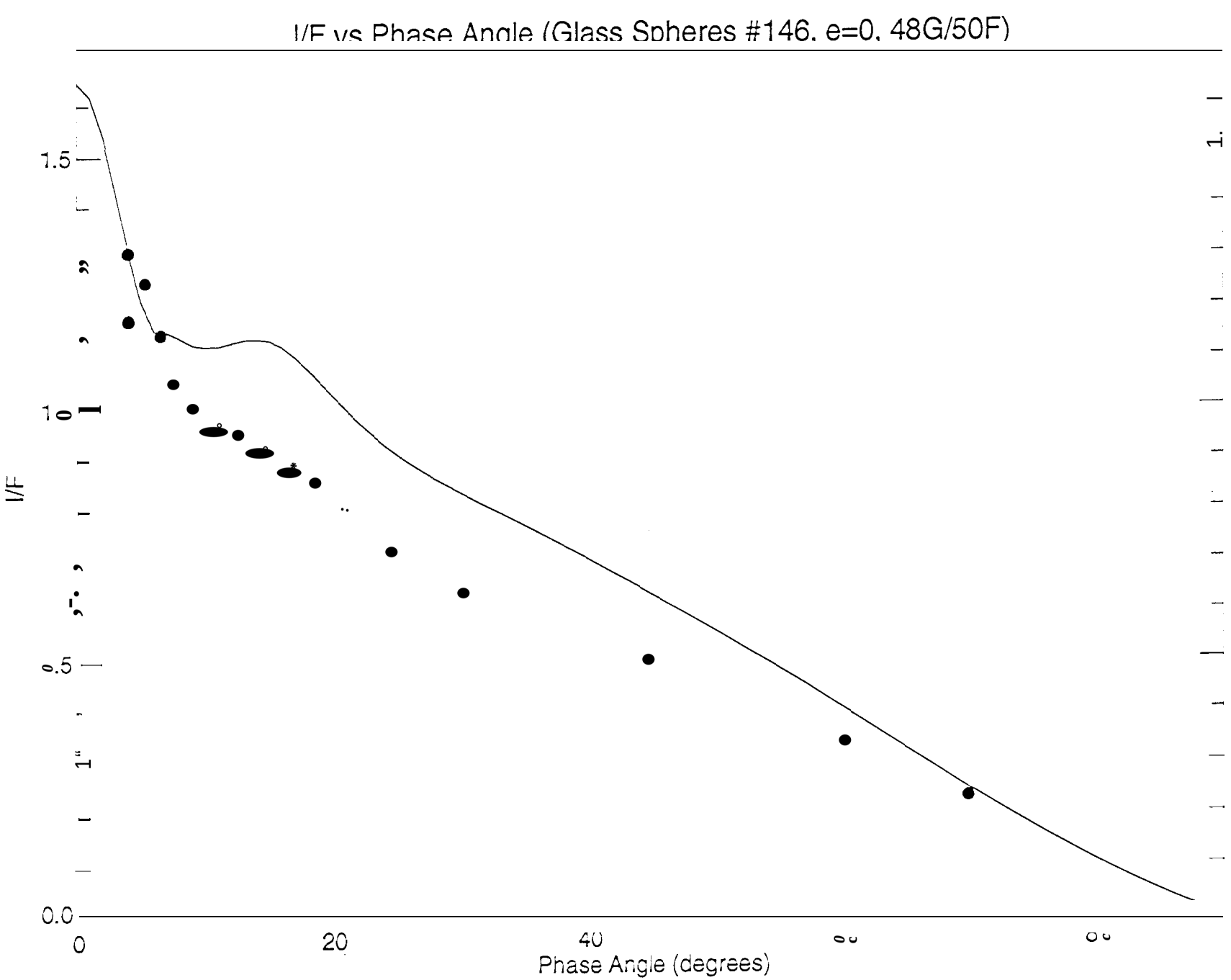
I/F vs Phase Angle (Glass Spheres #146, e=0, 48G/50F)
I/F
1.5
1.0
0.5
0.0
0
20
40
Phase Angle (degrees)

Fig 3a

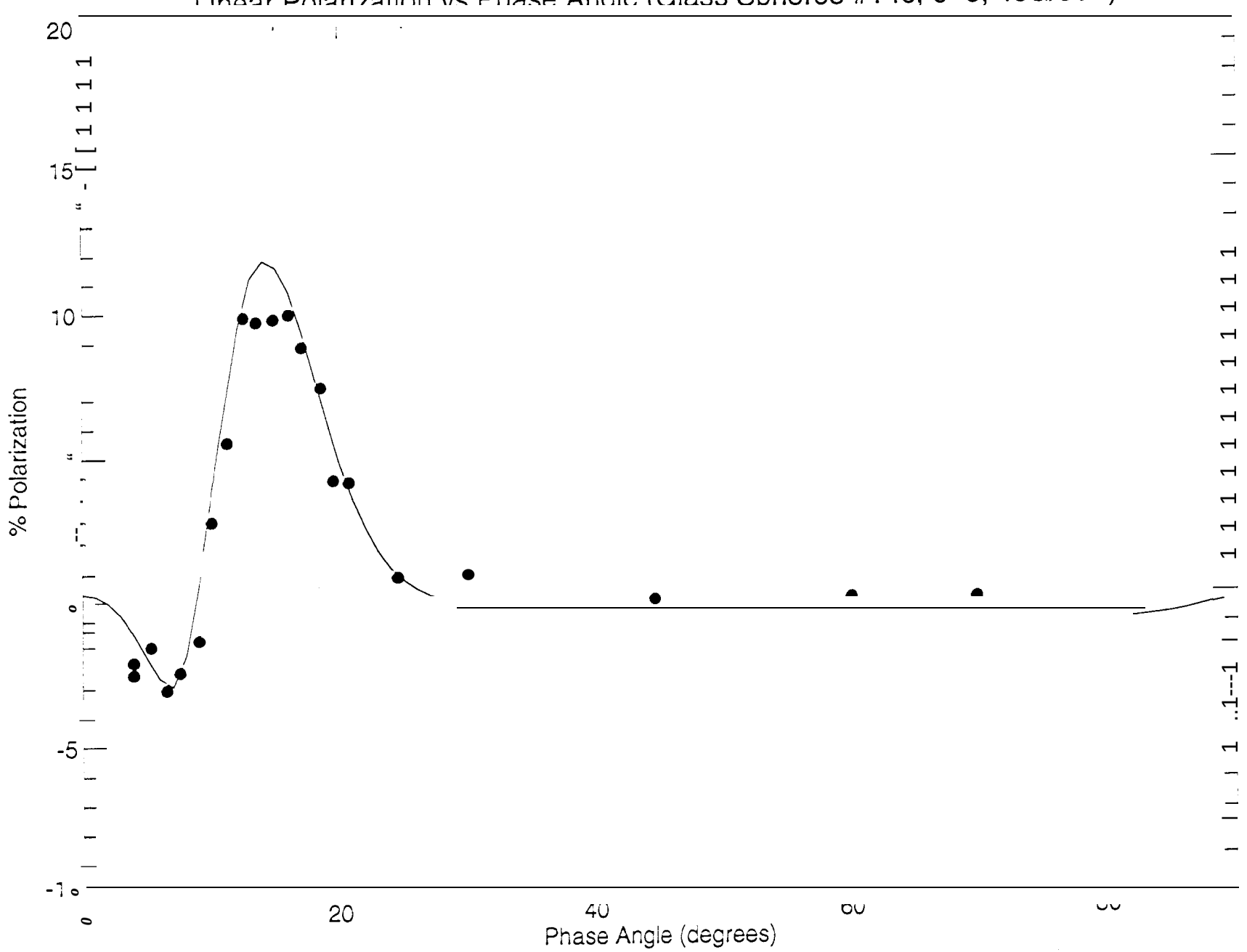
Linear Polarization vs Phase Angle (Glass Spheres #146, e=0, 48G/50F)
% Polarization
Phase Angle (degrees)
20
15
10
-5
-1
0
20
40
60

Fig. 3

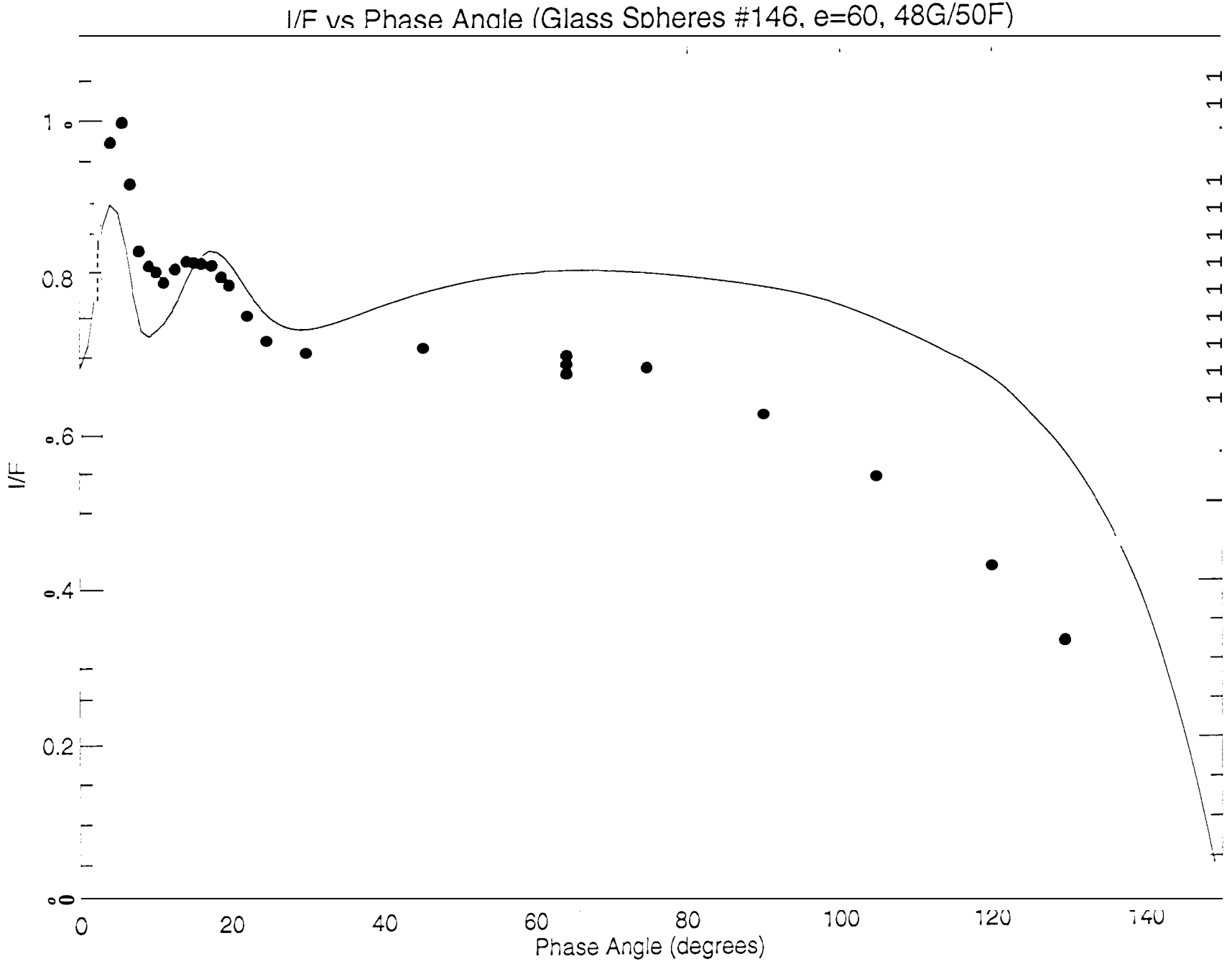
I/F vs Phase Angle (Glass Spheres #146, e=60, 48G/50F)
I/F
1.0
0.8
.6
.4
0.2
0
0
20
40
60
80
100
120
140
Phase Angle (degrees)

Fig. 3c

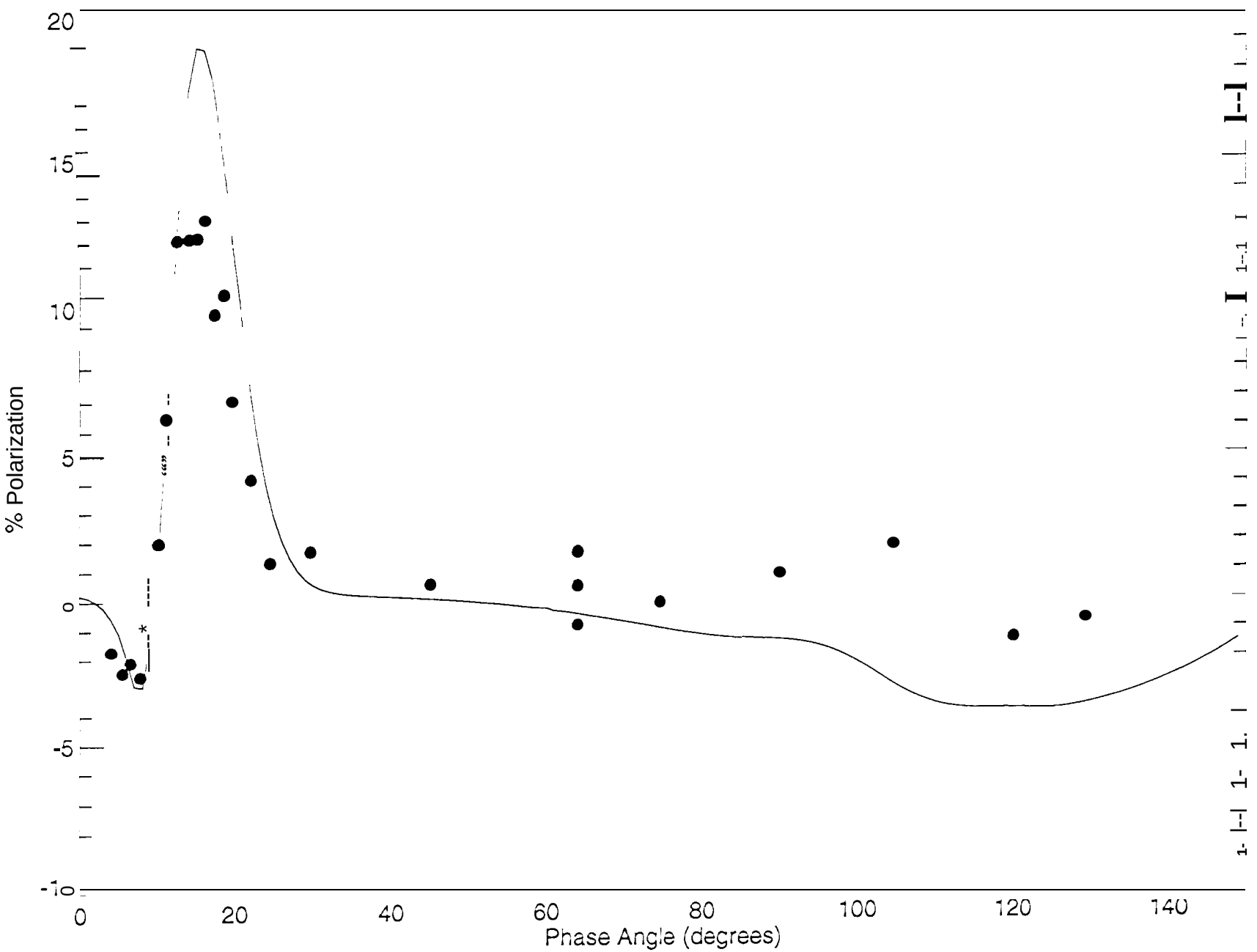
Linear Polarization vs Phase Angle (Glass Spheres #146, e=60, 48G/50F)
% Polarization
Phase Angle (degrees)
20
15
10
5
0
-5
-10
0
20
40
60
80
100
120
140

Fig. 3d

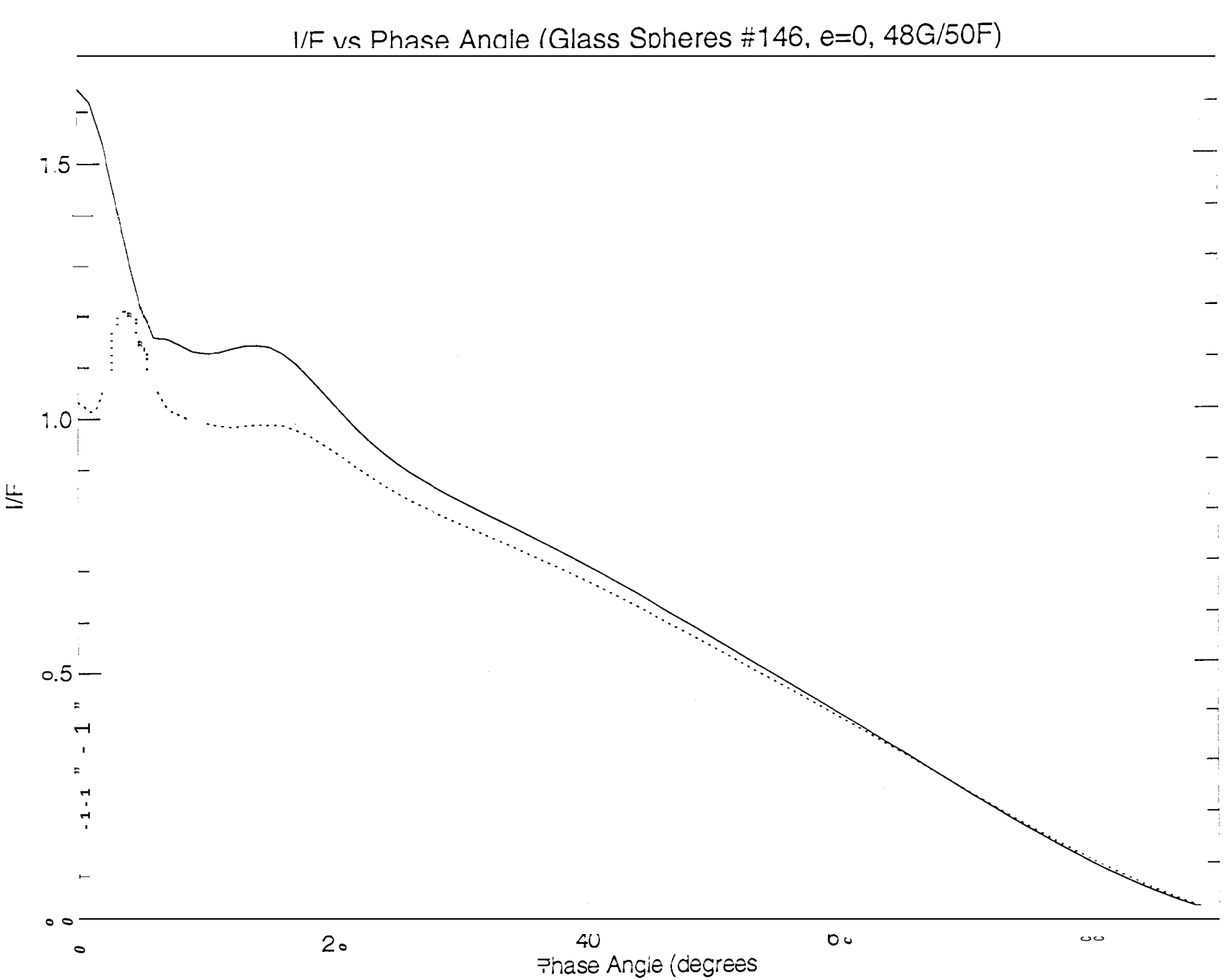
I/F vs Phase Angle (Glass Spheres #146, e=0, 48G/50F)
1.5
1.0
0.5
I/F
Phase Angle (degrees

Fig A1a

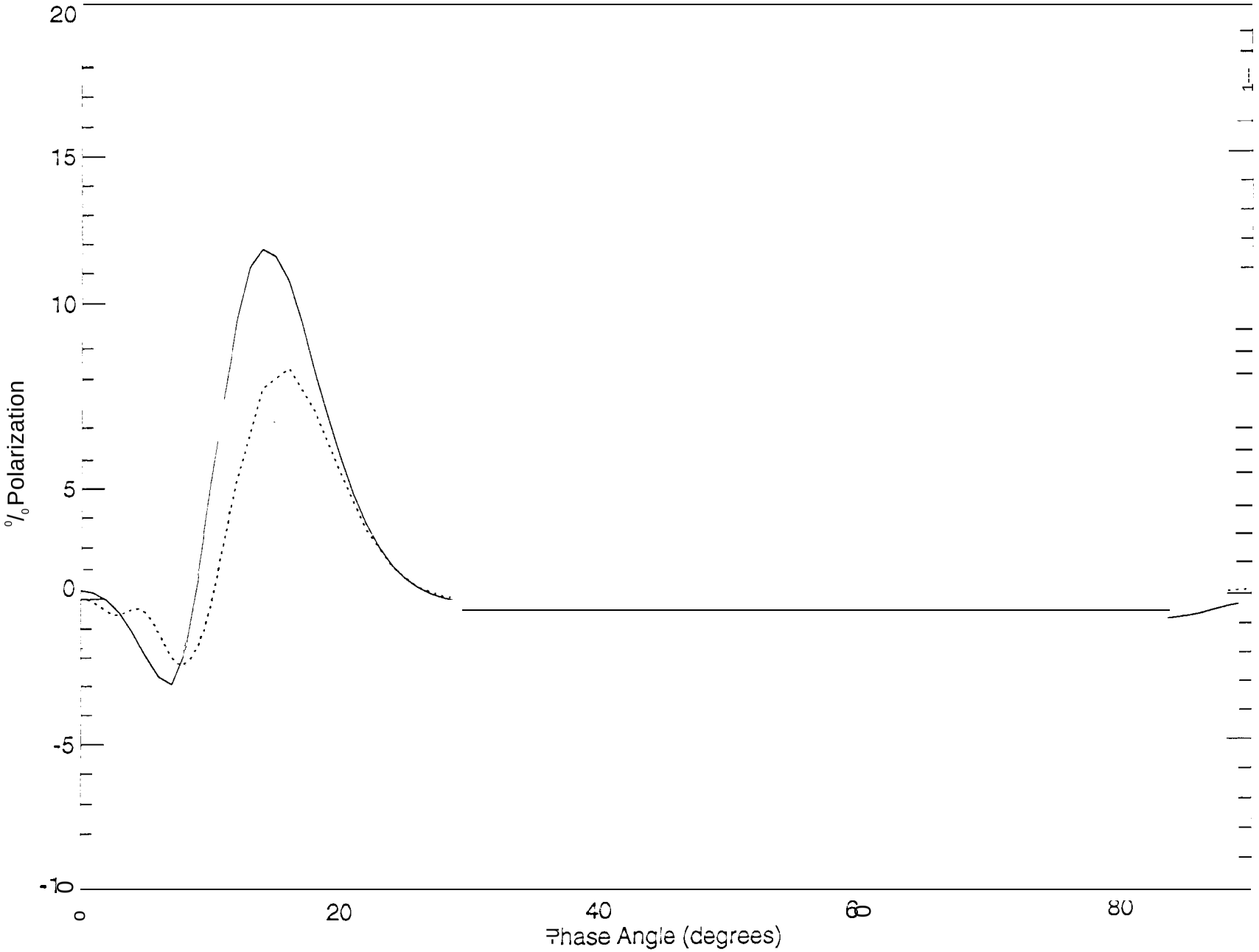
inear Polarization vs Phase Angle (Glass Spheres #146, e=0, 48G/50F)
20
15
10
5
0
-5
-10
% Polarization
0
20
40
60
80
Phase Angle (degrees)

Fig. A1b

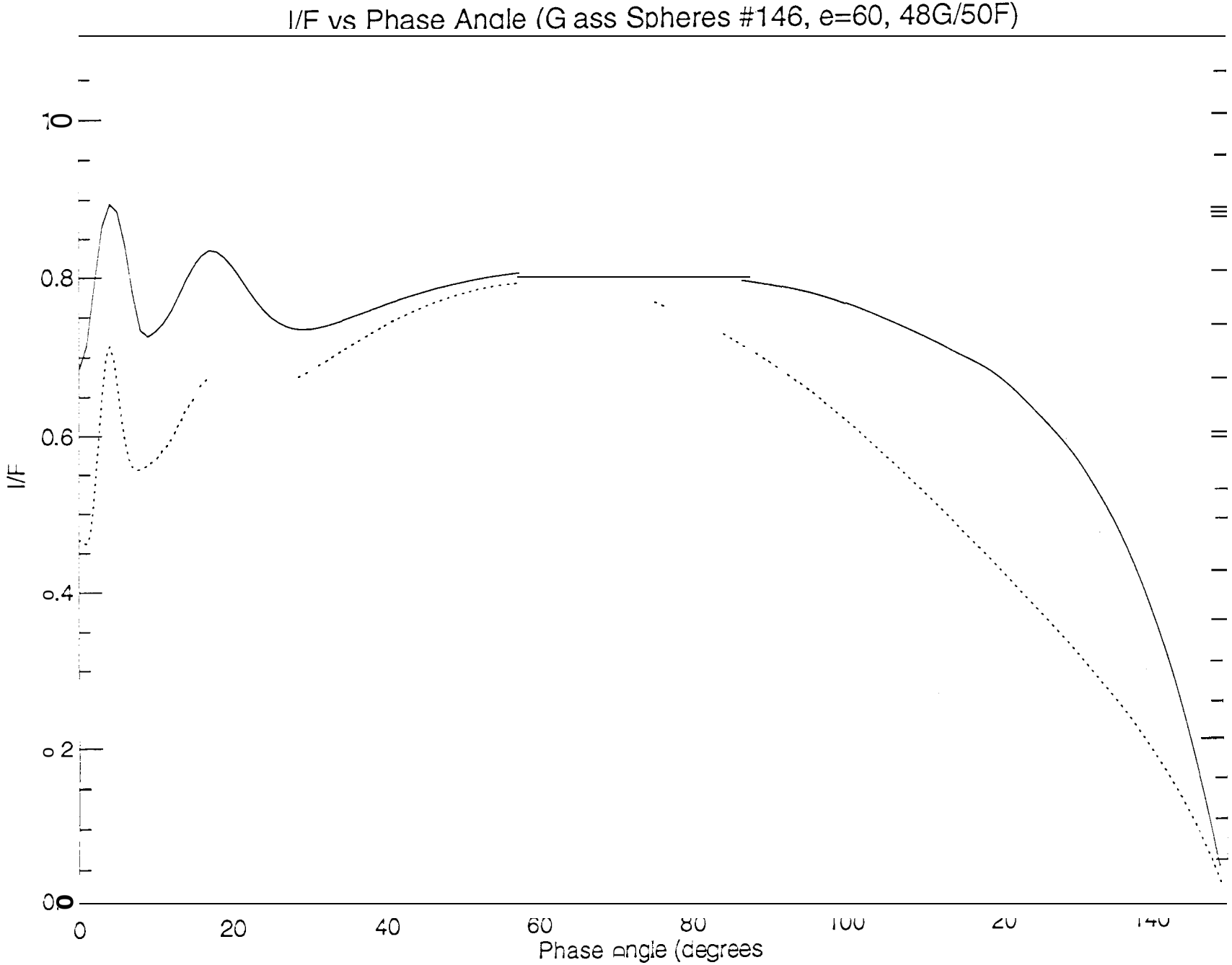
I/F vs Phase Angle (G ass Spheres #146, e=60, 48G/50F)
1.0
0.8
0.6
0.4
0.2
0.0
I/F
0
20
40
60
80
100
120
140
Phase angle (degrees

Fig. A1c

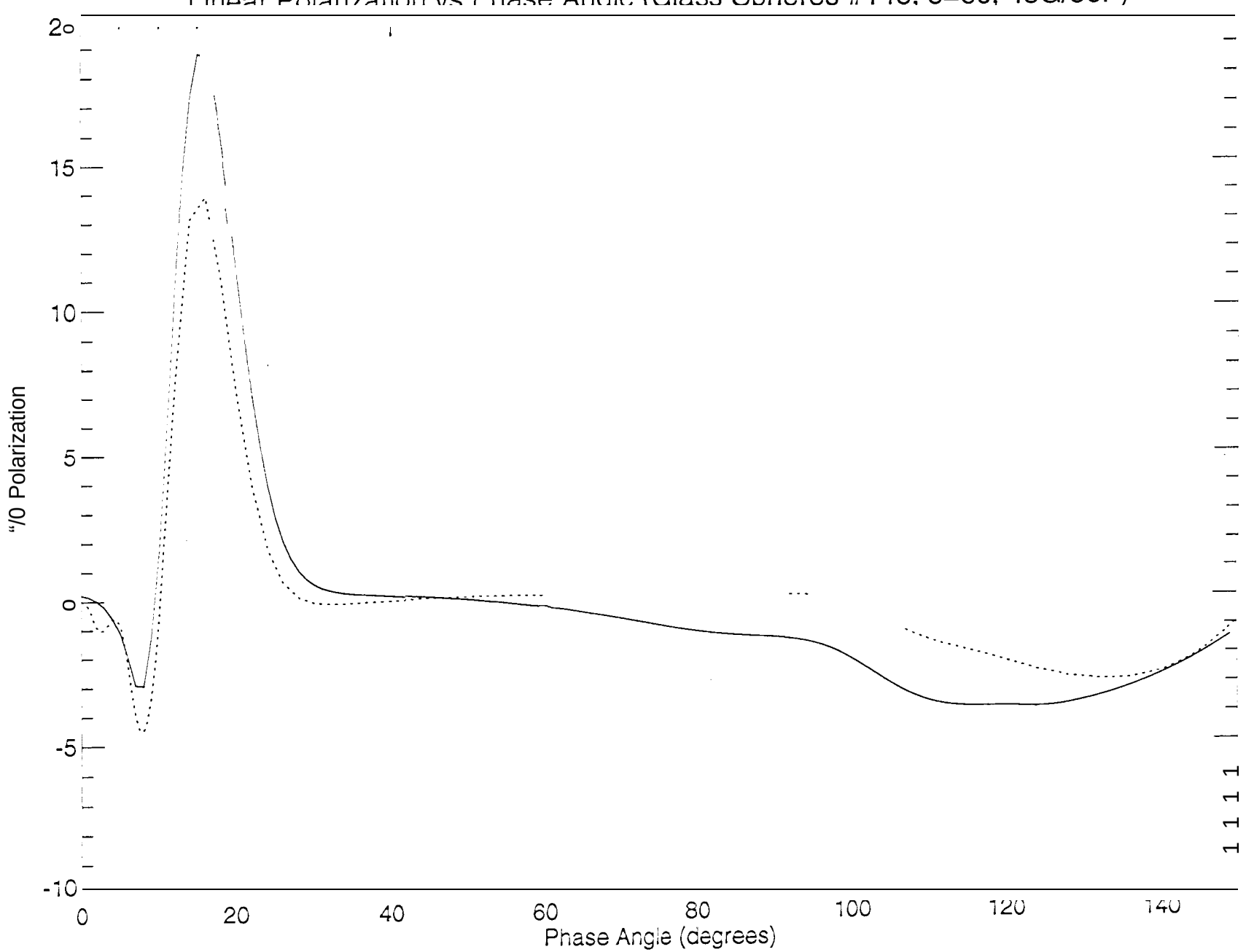
Linear Polarization vs Phase Angle (Glass Spheres #146, e=60, 48G/50F)
2o
15
10
5
0
-5
-10
"/0 Polarization
0
20
40
60
80
100
120
140
Phase Angle (degrees)

Fig. A1d